
Article:
Kalare, RS, Brooks, PC and Barton, DC orcid.org/0000-0003-4986-5817 (2016) Characterisation of a Carbon/Carbon Multi-Plate Clutch for a High Energy, Race Car Application. International Journal of Vehicle Performance, 2 (3). pp. 275-301. ISSN 1745-3208

https://doi.org/10.1504/IJVP.2016.078560

Characterisation of a Carbon/Carbon Multi-Plate Clutch for a High Energy, Race Car Application

Abstract

The torque output of a carbon/carbon multi-plate Formula One clutch during race starts has proved to be both unstable and inconsistent. A specially designed single clutch-plate interface dynamometer (SCID) showed the formation of narrow (~2mm), high-temperature (1300-1650℃) hot bands during tests replicating race start conditions, suggesting that less than 15% of the full friction surface areas were in contact. A thermomechanically coupled finite element analysis (TCFEA) was developed to simulate the thermomechanical behaviour of the clutch plates during SCID testing. With allowance for wear, the TCFEA closely replicated the SCID results. Both the SCID and TCFEA demonstrated no radial movement of the hot bands during single engagements indicating that torque instability is due to surface morphology effects alone. The hot band migration observed between successive SCID engagements indicated that torque inconsistency is due to both surface morphology and hot band migration effects.

Keywords: carbon/carbon, Formula One, F1, multi-plate clutch, torque instability, torque inconsistency, surface morphology, hot banding, thermoelastic instabilities, friction radius migration

1. Introduction

The basic structure of a carbon/carbon composite consists of a filler and matrix where the filler is carbon fibre and the matrix is a type of resin [1]. The matrix is combined with the carbon fibres into an uncured preform within a mold [2] which is then cured and subjected to pyrolysis to drive off non-carbon atoms. Further resin is impregnated into the porous composite by either liquid or gas deposition or infiltration methods. Both processes can take several days or even weeks. Several cycles of pyrolysis and impregnation are carried out before a final carbonisation stage which produces a composite that is almost entirely carbon and minimally porous. By using different resins and fibre precursors, with the fibres arranged in specific directions though the use of 2D or 3D weaves, along with careful control of the composite impregnation and carbonisation, carbon/carbon composites with specific properties can be produced for bespoke applications. The process of carbon/carbon composite production can take up to six months and hence is very expensive due to the energy demands. The clutch plates in this investigation are made up of polyacrylonitrile (PAN) carbon fibres impregnated using chemical vapour infiltration (CVI). Although the specific resin type is unknown, the composite is a commercially available product used in many race car brake and clutch applications.

Blanco et al. [3] present a literature review summarising research into carbon/carbon composite brake materials. They note that published papers are limited due to much of the research in this area being carried out by industry and many of the findings being protected by patents. This review also highlights that most published research is associated with the development of aircraft brakes, a point that is reiterated by Savage [4]. Aircraft brakes are similar in construction to the multi-plate carbon/carbon clutch used in this investigation in that friction is generated via disc-on-disc contact. The fact that they are also used in high energy applications such as aborted take-offs means that much of the research findings can be related directly to multi-plate clutches.

Gibson et al. [5] and Lawrence et al. [6] have both presented a brief history of the development of carbon/carbon composite multi-plate clutches for Formula One (F1) applications. The first carbon/carbon clutch was introduced in 1982 but it was not until 1987 that the first race victory using a carbon/carbon clutch was achieved. Carbon/carbon multi-plate clutches have since been standard technology within F1. The high coefficient of friction (COF) that the material offers, combined with its low density (offering weight saving opportunities) and high maximum operating temperature (>2000℃), make it an ideal clutch plate friction material for F1 applications.

The friction performance of carbon/carbon composite materials in ambient conditions has been investigated by several authors [3, 7, 8, 9] and the same general trends have been observed in relation to the variation of the friction coefficient with surface temperature. This, together with surface morphology examination, has enabled three distinct friction regimes to be identified. Initially the coefficient of friction is low as type I morphology (thin, smooth film) is dominant due to water being present in the friction surface. At approximately 150℃, the water is desorbed from the surface and a rapid increase in COF is observed (along with a rapid rise in temperature) as type II morphology (rough, powdery debris) is formed. As energy continues to be dissipated at the friction surface, type II morphology is converted to type III morphology (thick, smooth film). The COF falls from its peak value and remains fairly constant at a higher value than the COF at ambient temperature. The relationship between the surface morphology, COF and temperature is however more complex and the friction behaviour of carbon/carbon composites has also been shown to be strongly affected by the level of energy input [7, 10, 11, 12, 13], friction surface condition [14], ambient conditions [7, 9, 15, 16, 17] along with fibre type and orientation [18, 19, 20].

In sliding contact, the phenomenon of thermoelastic instabilities (TEI) can also have an effect on a friction material and its performance. Barber [21] states that any irregularities on the contacting surfaces of sliding solids will cause a non-uniform contact pressure distribution. The heat input distribution will mirror this non-uniformity and lead to preferential thermal expansion in the areas of high temperature. The contact pressure will then increase in these

areas, concentrating the heat input and causing further temperature increase and greater thermal expansion. The thermal distortion thus tends to exaggerate the original surface irregularities. Barber [21] also developed a computational model which showed that a height difference of as little as 1nm is sufficient to initiate TEI.

TEI may be initiated even if the friction surfaces are initially perfectly flat. Zhao et al. [22] and Abdullah et al. [23, 24] predicted contact localisation due to TEI in carbon/carbon multi-plate clutches using axisymmetric finite element models where the friction surfaces were modelled as initially perfectly flat with the heat flux input proportional to the coefficient of friction (COF), contact pressure and sliding velocity across the friction surface. Wear was not included in the models which predicted rapid contact loss at the inner and outer radii due to radial expansion of the clutch plates. Contact was then localised towards the centre of the friction surfaces leading to hot bands being formed. The simulations carried out by Zhao et al. [22] predicted hot bands between the central radii and the outer radii of the clutch plates. In contrast, Abdullah et al. [23, 24] predicted contact pressure localisation at the centre of the friction surfaces leading to the formation of central hot bands.

The differences in the contact pressure distributions predicted by Zhao et al. [22] and Abdullah et al. [23, 24] may be due to the fact that their respective axisymmetric models simulated several friction interfaces and so the expansion at one friction interface may affect the expansion of another leading to single contact pressure peaks and hot bands where the material properties affect the amount of expansion and hot band location.

The aim of the present investigation is to establish the cause of the unstable and inconsistent torque output of a carbon/carbon multi-plate clutch reported by many F1 teams. The following section describes the development of a unique dynamometer used to investigate in detail the performance of a single clutch-plate pair under typical race start conditions and the results of the dynamometer tests are presented in section 3. The development of a thermomechanically coupled finite element model is described in section 4 and the results for both analyses, with and without allowance for wear, are presented in section 5. Finally, in section 6 the combined

results of the experimental and numerical studies are discussed before the overall conclusions are summarised.

2. Single Clutch-Plate Interface Dynamometer (SCID)

A unique single clutch-plate interface dynamometer (SCID) was developed to facilitate friction and thermal performance testing of single clutch-plate pairs, eliminating the complexities of the full multi-plate clutch system. The SCID was designed to replicate typical race start rotational speeds, clamp loads and total energy dissipation levels. In the SCID, unlike in the race car where the initially stationary clutch plates (gearbox side) would be brought up the same speed as the rotating clutch plates (engine side) during the race start, one clutch plate in the clutch-plate pair is non-rotating and the rotating clutch plate is brought to rest. Figure 1 shows the overall layout of the SCID.

[FIGURE 1]

Once the main shaft has been spun up to speed, the mini-electromagnetic (EM) clutch situated between the driving shaft and main shaft is disengaged, decoupling the inertia of the driving shaft, intermediate shaft and electric motor. Only the kinetic energy stored in the known main shaft inertia will therefore be dissipated at the clutch-plate friction interface. The speed of rotation of the main shaft is measured using a shaft encoder ring with fifty holes equally spaced on a pitch circle diameter of Ø140mm and an infrared photoemitter.

The clutch-plate pair is engaged by pushing the non-rotating assembly (housed in linear bearings) forwards using the linear electric actuator. A lever arm is used to scale up the actuator output force. The in-line load cell measures the clamp load and a PID controller is used in conjunction with the actuator to regulate the clamp load. The torque generated at the clutch-plate interface causes the non-rotating assembly to rotate by a small angle, bringing the torque arm into contact with the load cell. The normal force measured is then converted to a torque value.

Thermocouples were unsuitable for measuring friction surface temperatures in this application for several reasons. Full area contact between the clutch plates eliminated the possibility of using sliding thermocouples whilst embedded thermocouples can only measure temperatures close to the friction surface but not the actual friction surface temperature itself. The inherent measurement lag of thermocouples also meant that any rapid transient thermal events may not have been captured. A FLIR X6540SC high-speed thermal imaging camera was therefore used to measure clutch-plate friction surface temperatures. The setup of the thermal imaging camera is shown in Figure 2.

[FIGURE 2]

A Ø12mm hole was machined through the non-rotating assembly and non-rotating clutch plate such that, via use of an infrared mirror set at a 45° angle, the friction surface of the rotating clutch plate could be viewed directly by the thermal imaging camera. The Ø12mm hole is centred at the mean geometric radius of the friction surface, which is 16mm wide, allowing 75% of the radial width of the friction surface to be imaged.

The FLIR X6540SC thermal imaging camera is able to measure temperatures of up to 1500℃ but cannot do so continuously from room temperature. The camera's 300-1500℃ temperature range was used in this investigation as high transient temperatures were anticipated. Due to the noise associated with using this temperature range, the lowest temperature that the camera was able to measure was 450℃. As the emissivity of the clutch-plate material was unknown, an emissivity value of 1 was assumed in order to process the results. An emissivity value of 1 represents an ideal black body and assumes that the object emits the maximum possible amount of radiation energy based on its surface temperature. This amount of radiation energy is measured by the thermal imaging camera and the object's surface temperature is calculated according to Planck's equation [25]. An emissivity value of 1 effectively produces the lowest possible temperatures that the clutch plate friction surfaces may achieve (i.e. a conservative measurement) as, if the clutch plate actually has an emissivity value of less than 1, it would need to have a higher surface temperature to emit the same amount of radiation energy as the assumed ideal black body. The true emissivity of the clutch

plates is likely to be close to unity as the black carbon/carbon material has a very dark appearance so the assumption of an ideal black body is reasonable.

Table 1 shows the combinations of initial rotational speed and clamp load investigated and the nomenclature used to identify these combinations throughout the paper. A new clutch-plate pair was used for each speed/load combination with seven consecutive clutch-plate engagements carried out for each pair. The clutch plates were allowed to cool for ten minutes between engagements. The speed/load combination that clutch-plate pair B4 was subjected to (8000rpm/1400N) is representative of typical race start conditions.

[TABLE 1]

3. SCID Results

For all the clutch-plate engagements carried out at the speed/load combinations listed in Table 1, continuous torque and temperature results were obtained, the most significant of which are discussed in the following sections.

3.1 Torque Output

Figures 3 and 4 show the torque outputs for clutch-plate pairs A2 and B4 which were respectively subjected to the lowest speed/load combination and highest speed/load combinations. For both figures, the first 0.8-1.0s of the time axis represents the build-up of the clamp load and hence the delay before the torque ramps up from zero at about 0.2s. At the low speed/load combination the torque output was both stable and consistent but at the high speed/load combination the torque output was both unstable during single engagements and inconsistent between engagements. It is important to note that the timescales for each figure are different and it can clearly be seen that the engagement times for the low speed/load combination tests were much higher than for the high speed/load combination. This is in essence the performance problem associated with the clutch in that stable, consistent torque

comes with the drawback of long engagement times but high torque, and hence short engagement times, result in unstable and inconsistent torque output behaviour. As either the initial rotational speed, clamp load or both were increased, the stability and consistency of the torque output was found to decrease.

[FIGURE 3]

[FIGURE 4]

In relation to the surface morphology regimes of the carbon/carbon clutch plates, the stable torque output shown in Figure 3 suggests a predominance of type I morphology resulting in a low COF throughout the engagement. This indicates that the power dissipation level at this particular low speed/load combination was insufficient to bring about a change from type I to type II morphology. The torque output behaviour shown in Figure 4 however suggests that the type I morphology has been converted to type II and then to type III. This indicates that the power dissipation level at this particular high speed/load combination was sufficient to initiate changes in surface morphology. This transitional behaviour was particularly evident during Engagement1 in Figure 4 where the torque output was initially low but rose sharply during the course of the engagement (at ~1.6s), indicating that type II morphology had formed which greatly increases the COF.

3.2 Temperature Measurements

The clutch-plate friction surface temperatures recorded by the thermal imaging camera showed three different, distinct temperature profiles. Figure 5 shows the clutch-plate friction surface temperature profile for Engagement4 at 7000rpm/1000N (A2) when the maximum temperature was recorded. The white circle superimposed on the image indicates the circumference of the Ø12mm viewing hole. Sp1 indicates the location of the innermost radial point viewed, Sp2 (label partially covered by the temperature scale) indicates the location of

the outermost radial point viewed and Sp3 indicates the point where the maximum temperature occurred.

[FIGURE 5]

It can clearly be seen from Figure 5 that the surface temperature profile at this point was non-uniform across the radial span of the friction surface. Towards the inner radius, the friction surface temperature was ~475℃ whilst the maximum temperature of ~550℃ occurred just beyond the mid-radius position. The temperature difference of around 75℃ is too small for the region of higher temperature to be classed as a distinct hot band.

The second type of surface temperature profile is shown in Figure 6 for Engagement7 at 7000rpm/1200N (A3) where the low temperature area across the radial span of the friction surface was the result of a cleaning groove in the clutch plates. The cleaning grooves are recessed from the friction surface and hence receive no direct heat input and remain at a low temperature throughout the engagement.

[FIGURE 6]

An additional marker (Sp4) has been added to Figure 6 as two areas of higher temperature were observed for this temperature profile. These two areas, each of around 650℃, were recorded towards the inner radius whereas the outer radius was at just above 450℃. These temperature differences are greater than those shown in Figure 5 for clutch-plate pair A2 and these two areas of high temperature observed for clutch-plate pair A3 could therefore be considered as two distinct low-temperature hot bands.

Figure 7 shows the third type of temperature profile for Engagement5 at 8000rpm/1400N (B4) when the maximum temperature was recorded. In contrast to the surface temperature profiles shown in Figures 5 and 6, Figure 7 clearly shows a distinct hot band on the clutch-plate friction surface. The extremely high temperatures (1300-1575℃) existed in a narrow band approximately 2mm wide where the temperatures outside of the band were at approximately only 500-600℃.

[FIGURE 7]

For all engagements carried out at the 7000rpm/1000N speed/load combination (A2), a similar surface temperature profile to that shown in Figure 5 was observed with maximum temperatures of 550℃-600℃. A similar surface temperature profile as that shown in Figure 7 was measured for all clutch-plate engagements carried out at 1400N for both speed combinations (A4 & B4) with maximum temperatures of 1300℃-1650℃. For the re maining speed/load combinations, a random mix of all three surface temperature profiles was observed.

The very high localised hot band temperatures observed during the clutch-plate engagement tests which were representative of race start conditions, suggest that the majority (if not all) of the friction work is being done in the areas of the hot bands. It is therefore reasonable to assume that the radial position of the hot band represents the location of an effective friction radius (EFR). Torque (T) is directly proportional to clamp load (P), COF (μ), and effective friction radius (r_e) (Equation 1) and hence if the EFR migrates, the torque output will vary even if the COF remains constant.

$$T = P\mu r_e \tag{1}$$

Figure 8 shows the evolution of the hot band shown in Figure 7. The hot band does not become visible to the thermal imaging system until 0.8s into the engagement indicating that the entire friction surface must be below 450℃ before this time. The surface temperature t hen increases before reaching a maximum temperature of 1573℃ at 1.16s (Figure 8e). The t emperature then falls and the width of the band increases to approximately 4mm from 2mm. This can be attributed to the rate of heat input becoming less than the rate of heat conduction away from the contact area as the engagement nears its end. The fluctuations in the temperature evolution could be due to surface morphology changes whereby type II and type III

morphology are in constant transition as discussed by Lee et al. [14]. This will cause changes in the friction surface COF and therefore affect the levels of power dissipation.

[FIGURE 8]

All clutch-plate engagements at 1400N (both speed values) exhibited a similar hot band evolution to that shown in Figure 8, which demonstrated that the hot bands, and hence EFR, do not migrate radially during a single clutch-plate engagement. However, the hot bands were observed to migrate between successive engagements to the extent that their radial location was different for all seven engagements. Figure 9 shows the hot band formed during Engagement1 at 8000rpm/1400N (B4). In comparison to Figure 7 which shows Engagement5, it can clearly be seen that the hot band, and hence EFR, is situated towards the inner radius. For this particular clutch plate design, the outer radius dimension is almost 50% greater than the inner radius dimension and hence if the EFR migrated from near the inner radius to near the outer radius between two successive engagements, an increase in torque output approaching 50% would result even if the surface morphology and hence COF remained constant.

[FIGURE 9]

The lack of EFR migration during single engagements showed that thermal expansion remains dominant during the very short engagement times. However, wear of the friction surfaces must occur for the EFR to migrate between successive engagements. The original contact point is worn away during the previous engagement but the level of wear is not sufficient to overcome the level of thermal expansion. The wear however then results in a surface recess once the clutch plates have cooled and this forces contact to be established elsewhere during the subsequent engagement.

4. Thermomechanically Coupled Finite Element Analysis (TCFEA)

The TCFEA was developed by coupling the commercially available software packages Matlab and Abaqus to simulate the mechanical and thermal response of the clutch plates during engagement tests. The first stage in the analysis was to construct an axisymmetric finite element model of the clutch plates in Abaqus. Figure 10 shows a schematic of the axisymmetric finite element model used. The analysis type used was coupled temperature displacement using quad CAX4T coupled temperature-displacement elements.

[FIGURE 10]

A bias ratio of 2.0 was used such that the mesh density in the axial direction was twice as dense at the friction surfaces than at the non-friction surfaces. Table 2 lists the material properties used in the finite element model. The material property values are linearly interpolated between the reference temperature values. Above the maximum reference temperature, the property value was assumed to remain constant due to the lack of any more detailed data. A mesh sensitivity analysis was carried out with the result that a mesh of 201 nodes in the radial direction and 21 nodes in the through-thickness direction (per clutch plate) was the best compromise between accuracy of results and computing time. An additional sensitivity analysis was carried out to determine the most appropriate time step value. A value of 0.01s was found to offer the best compromise between accuracy of results and computing time.

[TABLE 2]

A simple relationship between temperature and coefficient of friction was assumed in the analysis. These values, which have been taken from previous dynamometer tests, are listed in Table 3. As with the material properties, the COF values are linearly interpolated between the reference values and the COF is assumed to remain constant at a value of 0.5 at temperatures above 1200℃.

[TABLE 3]

4.1 Numerical Procedure

Before the full analysis was carried out, Matlab was used to modify the Abaqus input (.inp) file to assign an individual surface definition to each friction surface element, define each node on the slave friction surface as an individual set, assign heat flux inputs to each defined friction surface and add print commands to output contact pressure and temperature results for the defined nodes to the Abaqus data (.dat) file. After the input file was modified, the full analysis was carried out according to the procedure outlined in Figure 11. Further details of the numerical procedure are given in the appendix.

[FIGURE 11]

The friction surfaces were modelled as initially perfectly flat resulting in a uniform contact pressure across the friction interface at the start of the engagement. The initial speed and clamp load inputs used were 8000rpm and 1400N, replicating the typical race start speed/load combination (B4) investigated during the SCID engagement tests. The clamp load application was modelled to ramp up over a time period of one second as it did during SCID testing and the initial temperature of the clutch plates was set to 25℃ (298K). The an alysis was carried out until the relative rotational speed of the clutch plates was reduced to zero.

4.2 Wear Equation

The results of the SCID testing suggested that wear must occur in order for the effective friction radius to migrate between successive clutch-plate engagements. Zhao et al. [22] used a wear equation based on Archard's wear law [26] relating the amount of wear to contact pressure, sliding velocity and time:

$$\Delta h = kpu\Delta t \tag{2}$$

Where: Δh – Incremental Wear (m)

k – Wear Constant (m^2N^{-1})

p – Contact Pressure (Pa)

u – Sliding Velocity (ms^{-1})

Δt – Time Step (s)

However, it was also observed in the present SCID testing that wear tracks on the clutch plates became more apparent as the rotational speed and clamp load were increased and hence they also became more apparent as the maximum friction surface temperatures recorded increased. The actual wear mechanism is likely to have been due to abrasion, oxidation or, most likely, a combination of both. As oxidation wear would be expected to exponentially increase with temperature [5, 6, 17], an exponential term with relation to temperature was added to Equation 2 to give the wear equation used in the present TCFEA.

$$\Delta h = kpu\Delta te^{(Z/Z_o)} \tag{3}$$

Where: Z – Surface Temperature (K)

Z_o – Reference Temperature (K)

Surface characterisation of previously race-conditioned clutch plates showed waviness profiles had formed on the friction surfaces with an average height variation of ±1μm about the mean surface height. If this waviness profile was the result of hot banding, it was possible that 2μm of wear occurred during a single clutch-plate engagement. It was postulated that this incremental wear would occur during the period in which the maximum hot band temperatures occur. From the non-wear model results (discussed in section 5.1), the hot bands persisted for approximately 0.2s. The wear constant, k, was therefore calculated to be $6.25 \times 10^{-17} m^2 N^{-1}$ in order to give 2μm of wear in 0.2s at the hot band maximum temperature, contact pressure and sliding velocity at the radial location of the hot band.

The incremental wear calculated for each time step was then divided by the time step value to give a dimensional wear rate, w, during that time step as shown by Equation 4.

$$w = \frac{\Delta h}{\Delta t} \tag{4}$$

This wear rate was incorporated into the TCFEA through use of the adaptive meshing function in Abaqus. Using the velocity control method, each node along the friction interface was assigned an adaptive mesh definition during the stage of the process shown in Figure 11 when a new step is added. The velocity control method allows a velocity to be assigned to each

node such that the finite element model moves the node at that velocity to simulate wear whilst the node can still displace due to thermal and mechanical effects. The aggregate effects of wear, thermal expansion and mechanical loading are thus calculated for each node at the interface.

5. TCFEA Results

The TCFEA simulations were carried out first without any allowance for wear and then with allowance for wear according to the procedures discussed in section 4. The results of the TCFEA simulations are presented in the following sections.

5.1 Non-Wear Model

Figure 12a shows the contact pressure distribution and temperature profile across the friction interface after 0.15s when no allowance is made for wear. The clamp load has built up to only 210N by this point and hence the torque and heat flux input are still low. Despite this the analysis predicts a loss of contact and hence zero contact pressure at the inner and outer radii. The temperature profile is still uniform at this point.

[FIGURE 12]

The effect of this loss of contact at the inner and outer radii is to concentrate heat flux towards the centre of the friction interface which affects the temperature profile and hence the thermal expansion of the friction surfaces. The contact pressure distribution is then influenced by the non-uniform thermal expansion across the friction interface. Figure 12b shows the contact pressure distribution and temperature profile after 0.25s. Two areas of slightly higher contact pressure have been formed which are mirrored in the temperature profile as more heat is input to these areas.

Figure 12c shows the contact pressure distribution and temperature profile after 0.40s. The effect of the areas of high contact pressure and associated increased heat flux input to these areas has caused increased thermal expansion and localised temperature rises. Contact has been isolated to three areas with two distinct peaks of contact pressure arising either side of the friction surface centre along with a lower contact pressure peak at the centre. The temperature profile reflects the contact pressure distribution but is less pronounceddue to the effect of radial heat transfer.

Figure 13a shows the contact pressure distribution and temperature profiles after 0.78s when the maximum surface temperature occurs. Due to thermal expansion effects, contact has been isolated to the two areas of high contact pressure shown in Figure 12c. This results in two narrow bands of contact pressure as shown in Figure 13a leading to two high-temperature hot bands of ~1550℃ and ~1450℃ respectively.

[FIGURE 13]

Large temperature gradients exist in the clutch-plate through-thickness direction as well as along the friction interface as shown for both clutch plates in Figure 13b.

After the maximum friction surface temperature occurs at 0.78s, the heat flux input becomes less than the amount of heat conducted away from the high-temperature areas of the friction interface. As a result, the level of thermal expansion at the friction interface falls, lowering the contact pressure at the two localised contact points. Contact then begins to be re-established across the friction interface and the temperature gradients reduce in both the radial and through-thickness directions. Figures 14a and 14b illustrate this and show the contact pressure distribution and temperature profiles at the end of the simulated clutch-plate engagement (t=1.50s) when the relative rotational speed has reduced to zero.

[FIGURE 14]

5.2 Wear Model

The same finite element model and initial conditions were used for the wear simulation with only the addition of the adaptive mesh function to allow for wear of the surface nodes differentiating it from the non-wear simulations. Initially, the evolution of the contact pressure distribution and temperature profile across the friction interface was very similar for both simulations. However, as the clutch-plate engagement progressed, wear began to have an effect. Figure 15a shows the contact pressure distribution and temperature profile predicted by the wear model after 0.40s. In comparison to Figure 12, the three contact points causing the high pressure areas have been worn away and contact has been restricted to two areas close to the centre of the friction interface on either side of the centre. This results in two temperature peaks occurring close to each other, near to the centre of the friction interface.

[FIGURE 15]

Further wear then causes contact to move further towards the centre of the friction interface until contact is isolated virtually to a single contact area approximately 1mm wide as shown in Figure 15b. This results in the formation of a single narrow high-temperature hot band of approximately 1550℃ at the centre of the friction interface. The radial and through-thickness temperature gradients were similar to those shown in Figure 13 for the non-wear model.

After 0.77s when the maximum friction surface temperature occurs, the amount of heat input becomes less than the rate of heat conduction away from the contact area, both radially and in the through-thickness direction. As a result, the temperature of the hot band reduces and the width of the hot band increases as shown in Figure 15c. The reduced level of thermal expansion combined with wear of the single central contact area leads to two contact areas being re-established, resulting in the contact pressure and temperature distributions shown in Figure 15c.

In a similar fashion to the non-wear model, as the engagement progressed further, contact was re-established over an even larger area and the temperature gradients in both the radial and through-thickness direction reduce until the engagement is complete after 1.38s. The wear model predicts a slightly shorter engagement time than the non-wear model (t=1.50s) as

the average contact pressure arising from the single contact point predicted by the wear model is greater than the average contact pressure from the two contact points predicted in the non-wear model. As a result the average torque predicted by the wear model is higher than for the non-wear model and hence a shorter engagement time is predicted.

6. Discussion

The stable, consistent torque behaviour observed during the lowest speed/clamp load combination (Figure 3) suggests a predominance of type I surface morphology with no transition to type II morphology after water desorption. This is despite maximum friction surface temperatures of 550-600℃ measured on the friction surfaces. The tran sition from type I to type II morphology would be expected at 150℃. It is likely that be cause of the short engagement time, the friction surface has insufficient time at a high temperature to desorb all the water from the surface and the transition from type I to type II morphology cannot occur at this speed/load combination in this very short timescale.

As the clutch-plate friction surfaces will not be perfectly flat, contact will be localised to a number of surface asperities resulting from machining of the surfaces. The heat flux input will thus be concentrated to these contact points leading to a non-uniform temperature distribution. Increased thermal expansion in the areas of high temperature causes a further increase in contact pressure and hence heat flux input, exacerbating the effect until contact is completely localised to a few areas resulting in the formation of hot bands. The SCID results show that as the initial rotational speed and/or clamp load is increased, the power dissipation at the friction interface increases and the effect of hot banding becomes stronger.

The TCFEA analysis however predicts high levels of contact localisation and hot banding even when the friction surfaces of the clutch plates are modelled as initially perfectly flat. Initial contact loss at the inner and outer radii leads to contact pressure increases towards the centre of the friction interface. For the non-wear model this results in two contact points either side of

the centre of the friction interface leading to two distinct hot bands whereas the simulation including wear predicts a single centralised hot band. In this respect, the finite element model incorporating wear most closely replicates the SCID results.

The narrow, high-temperature hot bands (1300-1650℃) observed during SCID tests at the typical race start speed and load combination (8000rpm/1400N) indicate that a high degree of contact localisation occurs. The hot bands were measured to be approximately 2mm wide suggesting that as little as 12.5% of the friction surface areas may actually be in contact. Figure 16 shows the temperature profile for the TCFEA simulation incorporating wear at the time at which the maximum temperature occurred (0.73s). As with the SCID tests, the hot band was not observed to migrate radially.

[FIGURE 16]

As shown in Figure 16, the maximum hot band temperature predicted was ~1550℃ which is comparable with the hot band temperatures recorded during SCID testing for the same conditions (1300-1650℃). One limitation with the thermal imaging camera was that it could not measure temperatures below 450℃. Considering this cut-off temperature, Figure 16 shows the hot band to be approximately 2mm wide which again agrees with results from the SCID tests. However, as shown in Figure 15b, the actual contact area predicted by the TCFEA may momentarily be as little as 1mm wide.

The high degree of contact localisation during the race start condition SCID tests implies that the radial location of the hot band indicates an effective friction radius (EFR). The fact that neither the clamp load nor the EFR vary during a single engagement (according to both SCID and TCFEA results) shows that torque instability during a single engagement is due to surface morphology effects alone, leading to variations in COF (Equation 1). The torque inconsistency between engagements is however due to a combination of both surface morphology effects and effective friction radius migration. As well as influencing the EFR, if contact moves to a different area of the clutch-plate friction surface between successive engagements, it may move to an area with a different initial surface morphology. Dependent upon the structure of

the carbon/carbon composite in that particular area and previous conditioning, the surface morphology transition during the engagement may be markedly different to the previous engagement. This will in turn impact the COF and potentially result in unexpected torque output behaviour leading to a less than optimal race start.

The migration of the EFR between engagements observed during SCID tests indicates that wear of the friction surfaces is occurring. Without wear, the same contact point would persist between engagements and no EFR migration would occur. Due to the short clutch-plate engagement times (<3s), thermal expansion remains dominant over wear such that no EFR migration occurs during single engagements. However, once the clutch plates have cooled to ambient temperature, the wear that occurred at the previous contact point results in a surface recess; contact is thus established elsewhere during the next engagement which forces the change in EFR.

Both the twin-band temperature profile predicted by the non-wear TCFEA model and the single-band temperature profile predicted by the TCFEA model including wear were observed during SCID tests. The twin-band regime was observed only at much lower temperatures than for the single-band regime. The TCFEA wear model did predict the existence of two low-temperature hot bands as shown in Figure 15a before a single high-temperature hot band was formed as shown in Figure 15b. The two hot bands were predicted to have temperatures below 450℃ and as such would not be recorded by the thermal imaging camera. It is possible that this initial twin-band regime is therefore simply not observed even if it is occurring. It is also possible that the transition from the twin-band regime to the single-band regime occurs only above a certain temperature when wear becomes significant. The intermediate speed/load combinations between 7000rpm/1000N and 8000rpm/1400N used in the SCID tests may therefore represent transitional loading cases between wear being insignificant and becoming significant. This would account for the random nature of the temperature profiles observed at the intermediate loading cases where, if a certain potential trigger temperature was reached,

a single hot band was recorded; otherwise a twin-band regime or no distinct hot band was seen.

Zhao et al. [22] and Abdullah et al. [23, 24] predicted a single contact pressure/temperature peak despite no wear being included in their models whereas the TCFEA only predicted a single peak when wear was included. This difference may be the result of the TCFEA simulating only a single clutch-plate pair, and hence a single friction interface, whereas Zhao et al. [22] and Abdullah et al. [23, 24] simulated the full multi-plate aircraft clutch. The aggregate effect of TEI on all the friction surfaces may have resulted in a single contact area and hot band being predicted in their simulations even in the absence of any wear.

7. Conclusions

The phenomenon of thermoelastic instabilities has been shown to lead to the formation of hot bands on the friction surface of F1 carbon/carbon clutch plates. The high energy levels involved with this application resulted in narrow (~2mm) hot bands of very high maximum temperatures (1300-1650℃) being recorded during dynamometer tests representative of race start conditions.

The TCFEA confirmed the observed hot banding behaviour. At race start input levels, the TCFEA has shown that wear of the friction surfaces causes contact to be isolated to a single contact area resulting in a single, distinct, 2mm wide hot band with a maximum temperature of ~1550℃. These hot bands are formed despite the friction surfaces being initially perfectly flat.

The 2mm wide hot bands recorded during SCID testing suggested that as little as 12.5% of the friction surfaces are in contact but the TCFEA has predicted that, at least momentarily, it may be as small as 6.25% (1mm contact width) leading to the narrow high-temperature hot bands observed in the SCID tests and predicted by the TCFEA..

The narrow high-temperature hot bands affect the location of the effective friction radius. The SCID has shown that hot bands do not migrate during single clutch-plate engagements but do migrate between successive clutch-plate engagements. The clutch-plate torque output instability during single engagements is therefore due to surface morphology effects alone whilst the torque output inconsistency between successive engagements is due to a combination of both surface morphology effects and effective friction radius migration.

The TCFEA confirmed that the effective friction radius does not migrate significantly during a single engagement and therefore has little influence on any torque output instability of the clutch-plate pair. These findings have important implications for the design and setup conditions of carbon/carbon clutches for F1 race cars.

The TCFEA has also shown that thermal expansion remains dominant over wear during the short single engagement times and thus the EFR does not migrate during single engagements as observed during SCID tests. The migration of the EFR between successive engagements observed during the SCID tests can only occur if wear has eliminated the original contact point resulting in contact being established elsewhere.

References

[1] Inagaki, M., New Carbon: Control of Structure and Functions. First Edition, Oxford, Elsevier Science Ltd., 2000, ISBN 9780080525709

[2] Strong, A.B., Fundamentals of Composites Manufacturing, Second Edition, Dearborn, Michigan, Society of Manufacturing Engineers, 2008, ISBN 9780872638549

[3] Blanco, C., Bermejo, J., Marsh, H., Menendez, R., Chemical and physical properties of carbon as related to brake performance, Wear, 1997, Vol. 213, Issues 1-2, pp.1-12

[4] Savage, G., Formula 1 Composites Engineering, Engineering Failure Analysis, 2009, Vol. 17, pp.92-115

[5] Gibson, D.W., Taccini, G.J., Carbon/Carbon Friction Materials for Dry and Wet Brake and Clutch Applications, Peoria, Illinois, April 11-13, 1989, SAE Technical Paper, 890950

[6] Lawrence, G., Mace, G., Bowler, N., Goddard, G., Morrey, D., Measurement of the Interfacial Plate Temperature within a Carbon Clutch and Determination of Effects upon its Friction Characteristics, Motorsports Engineering Conference & Exhibition,

Dearborn, Michigan, December 5-7, 2006, SAE Technical Paper 2006-01-3636, Warrendale, Pennsylvania, USA, 2006

[7] Yen, B.K., Ishihara, T., An Investigation of Friction and Wear Mechanisms of Carbon-Carbon Composites in Nitrogen and Air at Elevated Temperatures, Carbon, 1996, Vol. 34, No.4, pp.489-498

[8] Krkoska, M., Filip, P., Humidity and Frictional Performance of C/C Composites, Developments in Advanced Ceramics and Composites: Ceramic Engineering and Science Proceedings, 2008, Vol. 26, No.8, Chapter 17

[9] Kasem, H., Bonnamy, S., Berthier, Y., Dufrenoy, P., Jacquemard, P., Tribological, physiochemical and thermal study of the abrupt friction transition during carbon/carbon composite friction, Wear, 2008, Vol. 267, pp. 846-852

[10] Kasem, H., Berthier, Y., Bonnamy, S., Jacquemard, P., Influence of sliding speed on wear of C/C composites under different controlled contact temperatures, 6th European Conference on Braking, Lille, France, 2010

[11] Yen, B.K., Ishihara, T., The Surface Morphology and Structure of Carbon-Carbon Composites in High-Energy Sliding Contact, Wear, 1994, Vol. 174, pp.111-117 237

[12] Hutton, T.J., McEnaney, B., Crelling, J.C., Structural studies of wear debris from carbon-carbon composite aircraft brakes, Carbon, 1998, Vol. 37, pp.907-916

[13] Francois, M., Joly, J.P., Kapsa, P., Jacquemard, P., A temperature-programmed desorption and oxidation investigation of wear debris from carbon/carbon composite aircraft brakes, Carbon, 2007, Vol. 45, pp. 124-131

[14] Lee, K.J., Kuo, H.H., Chern Lin, J.H., Ju, C.P., Effect of surface condition on tribological behavior of PAN-CVI based carbon-carbon composite, Materials Chemistry and Physics, 1999, Vol. 57, pp.244-252

[15] Chen, J.D., Chern Lin, J.H., Ju, C.P., Effect of humidity on the tribological behavior of carbon-carbon composites, Wear, 1996, Vol. 193, pp.38-47

[16] Tanner, J.A., Travis, M., Adsorption and Desorption Effects on Carbon Brake Material Friction and Wear Characteristics. Aerotech Congress & Exhibition, Grapevine, Texas, October 3-6, 2005, SAE Technical Paper 2005-01-3436, Warrendale, Pennsylvania, 2005

[17] Yen, B.K., Ishihara, T., On Temperature-Dependent Tribological Regimes and Oxidation of Carbon-Carbon Composites up to 1800℃, Wear, 1996, Vol. 196, pp .254-262

[18] Byrne, C., Wang, Z., Influence of Thermal Properties on Friction Performance of Carbon Composites, Carbon, 2001, Vol.39, pp.1789-1801

[19] Hutton, T.J., Johnson, D., McEnaney, B., Effects of fibre orientation on the tribology of a model carbon-carbon composite, Wear, 2001, Vol. 249, pp.647-655

[20] Hao, M., Luo, R., Hou, Z., Yang, W., Xiang, Q., Yang, C., Effect of fiber-types on the braking performances of carbon/carbon composites, Wear, 2014, Vol. 319, pp. 145-149

[21] Barber, J.R., Thermoelastic Instabilities in the Sliding of Conforming Solids, Proceedings of the Royal Society of London, Series A, Mathematical and Physics, 1969, Vol.312, No.1510, pp.381-394

[22] Zhao, S., Hilmas, G.E., Dharani, L.R., Behavior of a composite multi-plate clutch subjected to mechanical and frictionally excited thermal load, Wear, 2008, Vol. 264, pp.1059-1068

[23] Abdullah, O.I., Al-Sahb, W.A., Al-Shabibi, A.M., THERMOELASTIC ANALYSIS OF MULTI-DISC CLUTCHES USING FINITE ELEMENT METHOD, Tribologia, 2014, Vol.5, pp. 9-24

[24] Abdullah, O.I., Akhtar, M.J., Schlattmann, J., Investigation of Thermo-Elastic Behavior of Multidisk Clutches, Journal of Tribology, 2015, Vol. 137, pp. 1-9

[25] Williams, T., Thermal Imaging Cameras: Characteristics and Performance, Taylor & Francis, 2009, ISBN 9781420071863

[26] Archard, J. F., Contact and Rubbing of Flat Surfaces, Journal of Applied Physics, 1953, Vol. 24, pp.981-988

Appendix

The following section provides further details of the numerical process discussed in Section 4.1 for the thermomechanically coupled finite element analysis (TCFEA).

Once the Abaqus job is complete, the Matlab program opens and scans the Abaqus .dat file for the printed results for a particular node. This is done in a loop such that the contact pressure result for a single node is read and stored in a matrix within Matlab. This process is then repeated for the other nodes, adding the results to the existing matrix. The same is then done for the temperature results.

The COF values are used to calculate the torque produced at the friction interface. The overall value of torque produced is calculated by summing the torque produced at each element pair along the friction interface according to Equation A1:

$$T = \sum T_e \tag{A1}$$

The torque at each element pair is calculated using Equation A2:

$$T_e = p_e \times A_e \times COF_e \times r_e \tag{A2}$$

Where: T_e – Torque Generated by Element Pair (Nm)

p_e – Mean Contact Pressure Across Element Pair (Pa)

A_e – Annular Area of Element Pair (m^2)

COF_e – Coefficient of Friction

r_e – Mean Radius of Element Pair (m)

The contact pressure is output only at the friction surface nodes of the slave surface (rotating clutch plate) so the contact pressure for the element pairs was calculated by taking the average of the contact pressure values at the surface nodes of the elements. The COF value was taken as the average of the COF values calculated for the two surface nodes based on their temperatures. It can be seen from Equation A2 that torque can only be produced if there is contact pressure meaning that no torque can be generated where the friction surfaces have separated. The effective friction radius (EFR) is calculated separately from the torque using Equation A3 using the contact pressure and radius values at each node:

$$EFR = \frac{\sum(r_n \times p_n)}{\sum p_n} \tag{A3}$$

The total torque generated at the friction interface is then used to calculate the decrease in rotational speed of the rotating clutch plate and associated inertia according to Newton's second law of motion.

$$T = I\dot{\omega} \tag{A4}$$

$$\omega_2 = \omega_1 - \dot{\omega}\Delta t \tag{A5}$$

Where: I – Inertia (kgm^2)

$\dot{\omega}$ – Rotational Deceleration (rads^{-2})

$\omega_{1,2}$ – Initial/Final Rotational Speed (rads^{-1})

Δt – Time Step (s)

This in turn allows calculation of the energy dissipation at the friction interface during the next time step, equal to the reduction in kinetic energy of the rotating mass. This value is divided by the clutch plate friction surface area to obtain an overall heat flux input value. However, the

total heat flux is then partitioned according to the contact pressure distribution across the friction interface which reflects the fact that no torque can be produced without contact and therefore no energy will be dissipated at those points. The first stage in calculating the distribution of heat flux involves calculating a contact pressure ratio for each element using Equations A6 and A7:

$$p_{avg} = \frac{\sum p_n}{N} \tag{A6}$$

$$R_e = \frac{p_e}{p_{avg}} \tag{A7}$$

Where: N – Number of Nodes Along Friction Interface

R_e – Contact Pressure Ratio of Element Pair

The heat flux input at each element pair along the friction interface is then calculated:

$$q_e'' = q'' \times R_e \tag{A8}$$

Where: q'' – Overall Heat Flux Input (Wm^{-2})

q_e'' – Heat Flux Input to Each Element Pair (Wm^{-2})

Once the heat flux distribution has been calculated, a new step is appended to the .inp file with a new step name and the new values of heat flux input defined. The process represented by Figure 11 is repeated using a ‘for’ loop until the rotating clutch plate has become stationary at which point a break command forces Matlab to exit the ‘for’ loop. The results of the analysis are saved to text files which can then be read by Matlab using scripts that have been written specifically to present the results.

Initial rpm/Total Energy Dissipation (kJ)	Clamp Load (N)		
	1000	**1200**	**1400**
7000/6.74	A2	A3	A4
8000/8.80	B2	B3	B4

Table 1 – Initial Rotational Speed/Clamp Load Combinations Used in SCID Tests

Property	**Temperature (℃)**	**Property Value**
Density (kgm^{-3})	All	1850
Young's Modulus (Nm^{-2})	All	$17.5x10^{9}$
Thermal Conductivity ($Wm^{-1}K^{-1}$)	25	10.5
	300	14.3
	600	14.9
Specific Heat Capacity ($Jkg^{-1}K^{-1}$)	25	708
	300	1350
	500	1730
	600	1720
Expansion Coefficient	All	$1.6x10^{-6}$

Table 2 – Material Property Reference Values Used in TCFEA

Temperature (℃)	**COF**
25	0.20
200	0.25
400	0.30
600	0.35
800	0.40
1000	0.45
1200	0.50

Table 3 – Temperature-COF Reference Values Used in TCFEA

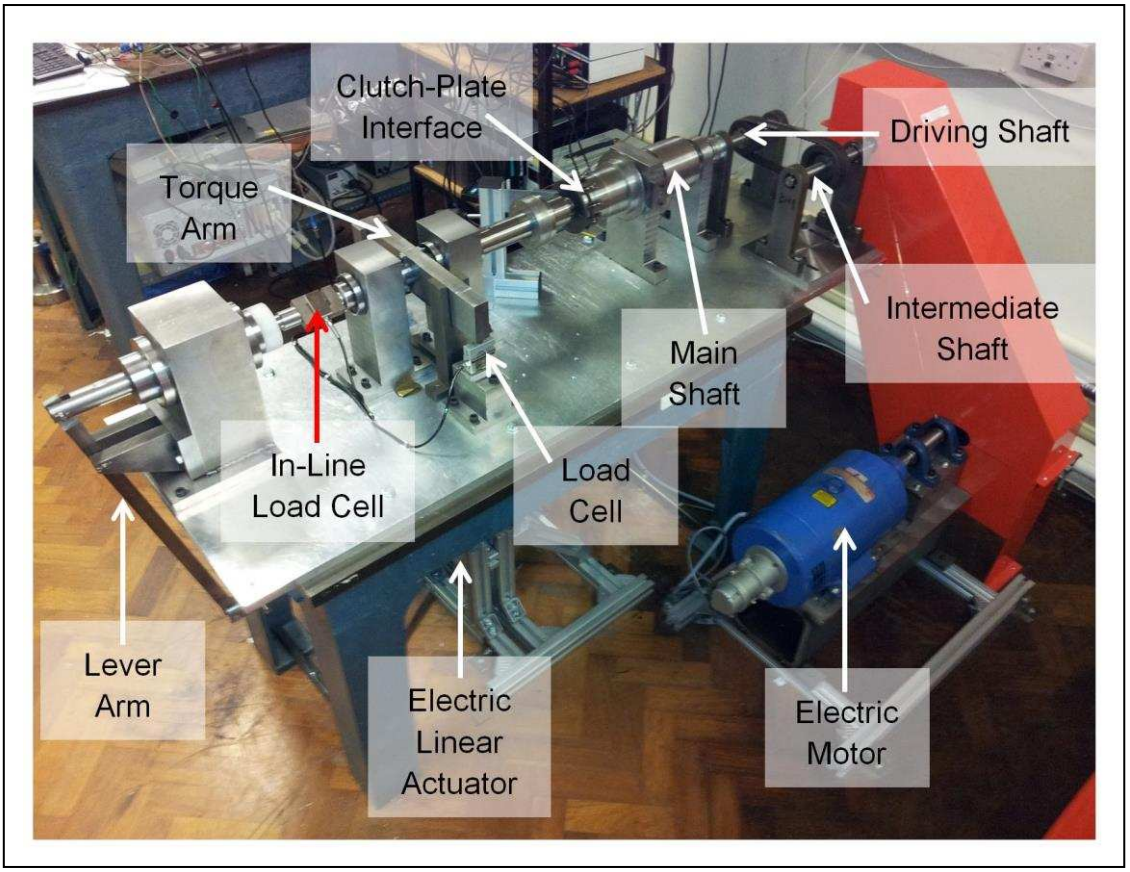

Figure 1 – SCID Layout

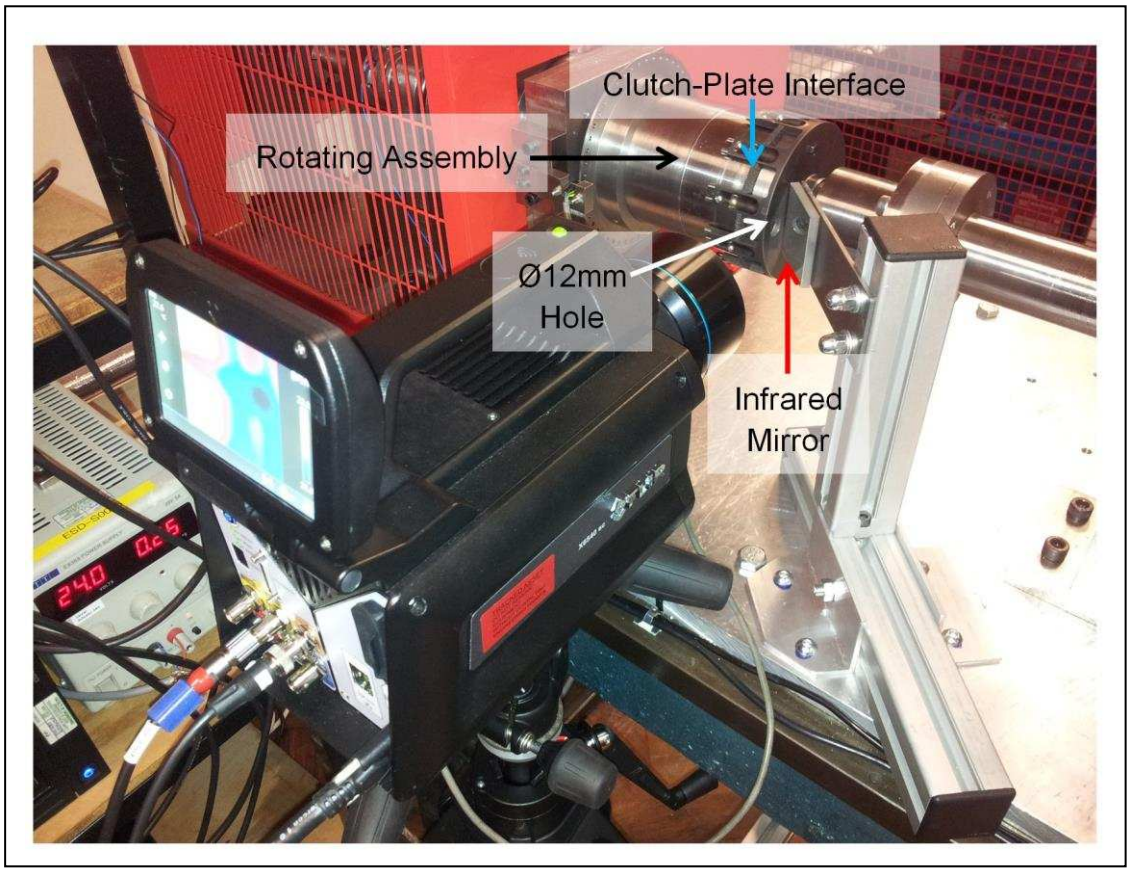

Figure 2 – Thermal Imaging Camera Setup for SCID

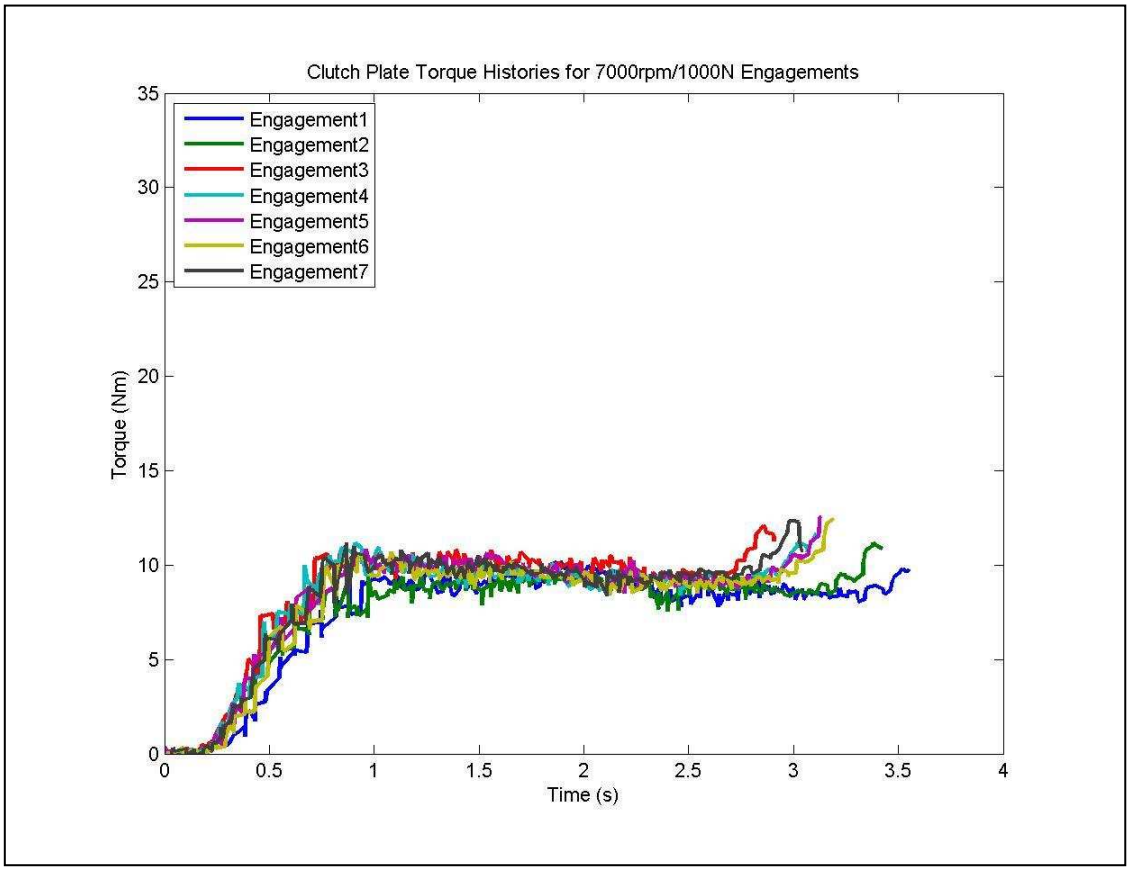

Figure 3 – SCID Torque Output Results for 7000rpm/1000N Speed/Load Combination (A2)

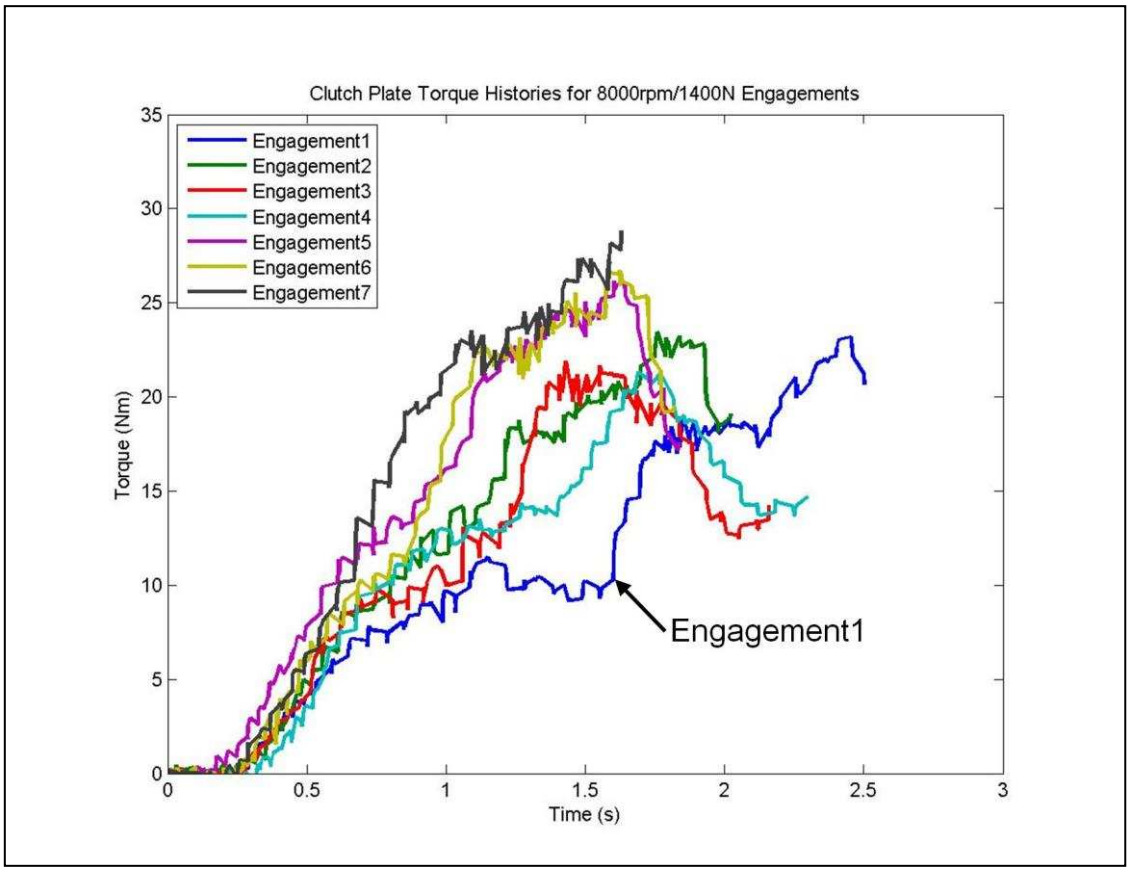

Figure 4 – SCID Torque Output Results for 8000rpm/1400N Speed/Load Combination (B4)

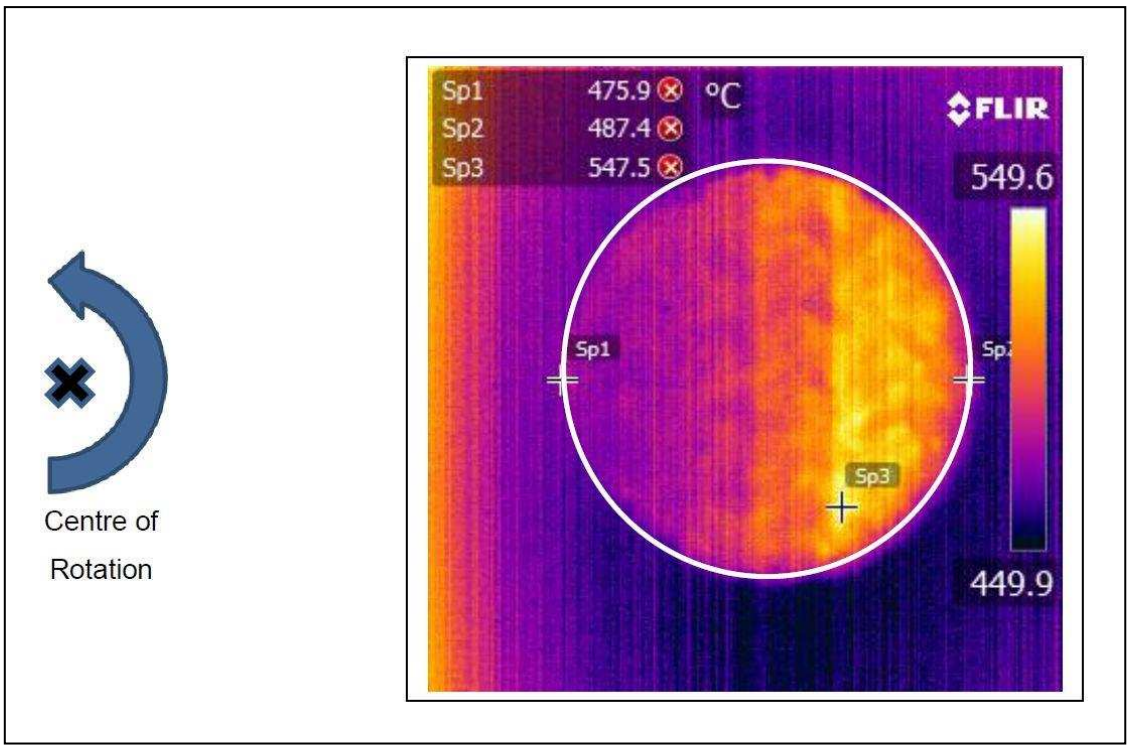

Figure 5 – Maximum Clutch-Plate Friction Surface Temperature Recorded During Engagement4 at 7000rpm/1000N Speed/Clamp Load Combination (A2)

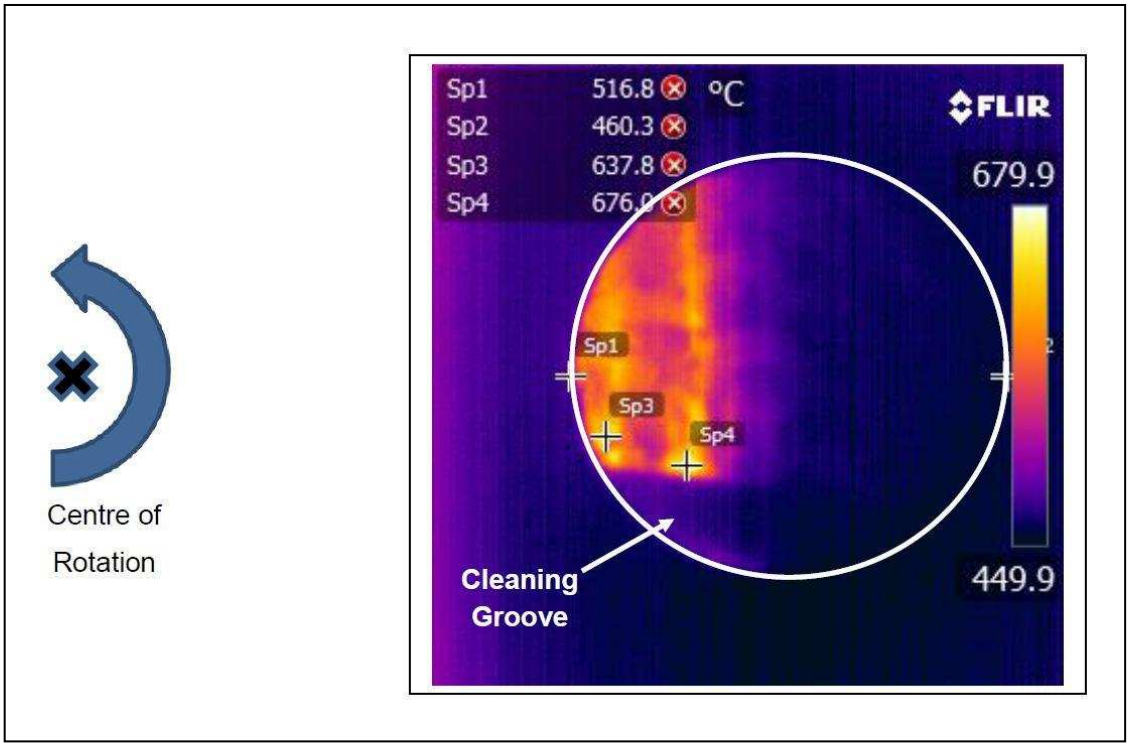

Figure 6 – Maximum Clutch-Plate Friction Surface Temperature Recorded During Engagement7 at 7000rpm/1200N Speed/Load Combination (A3)

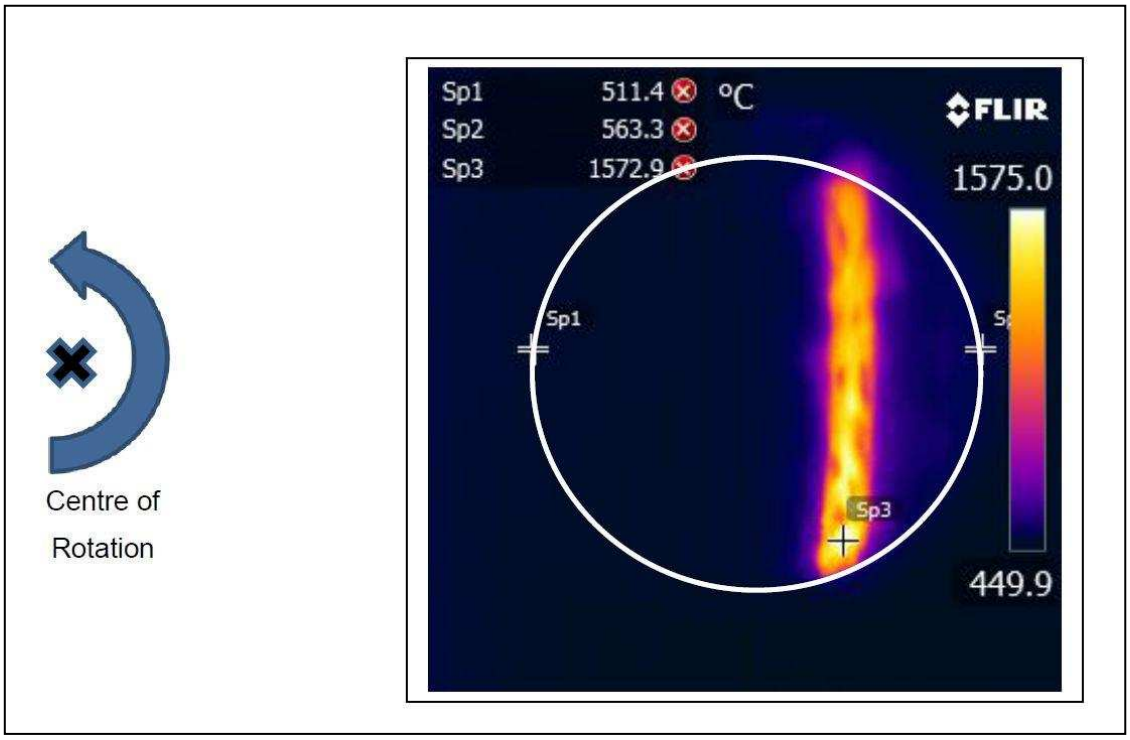

Figure 7 – Maximum Clutch-Plate Friction Surface Temperature Recorded During Engagement5 at 8000rpm/1400N Speed/Clamp Load Combination (B4)

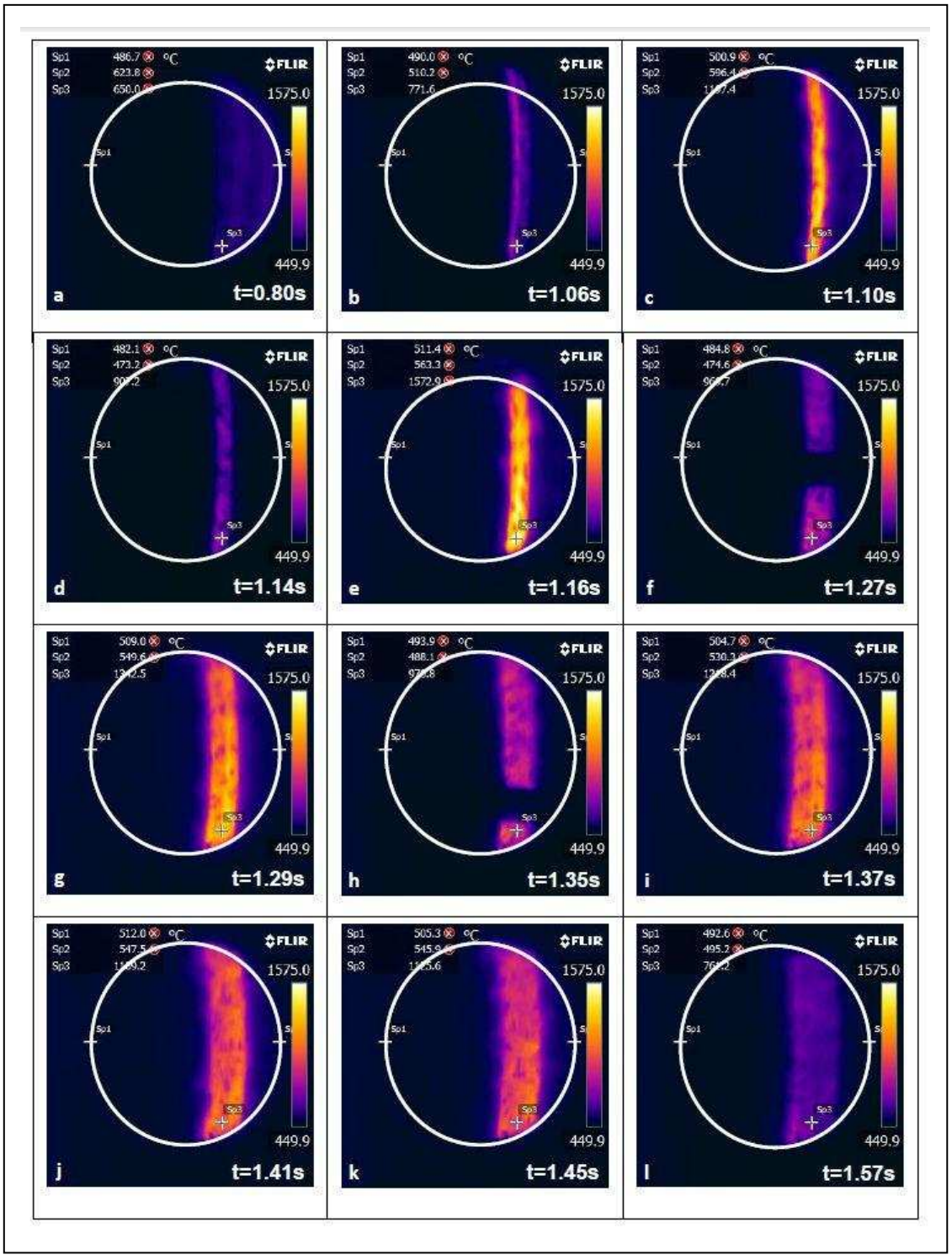

Figure 8 – Hot Band Evolution During Engagement5 at 8000rpm/1400N (Typical of Race Start) Speed/Clamp Load Combination (B4)

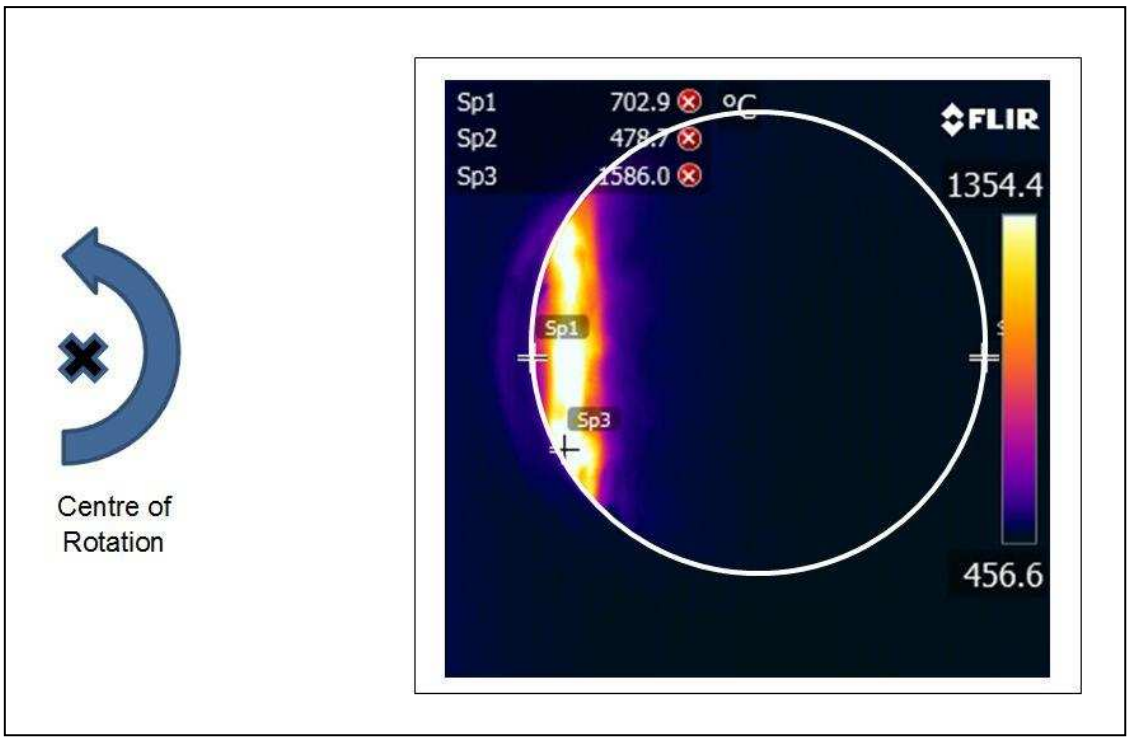

Figure 9 – Maximum Clutch-Plate Friction Surface Temperature Recorded During Engagement1 at 8000rpm/1400N Speed/Clamp Load Combination (B4)

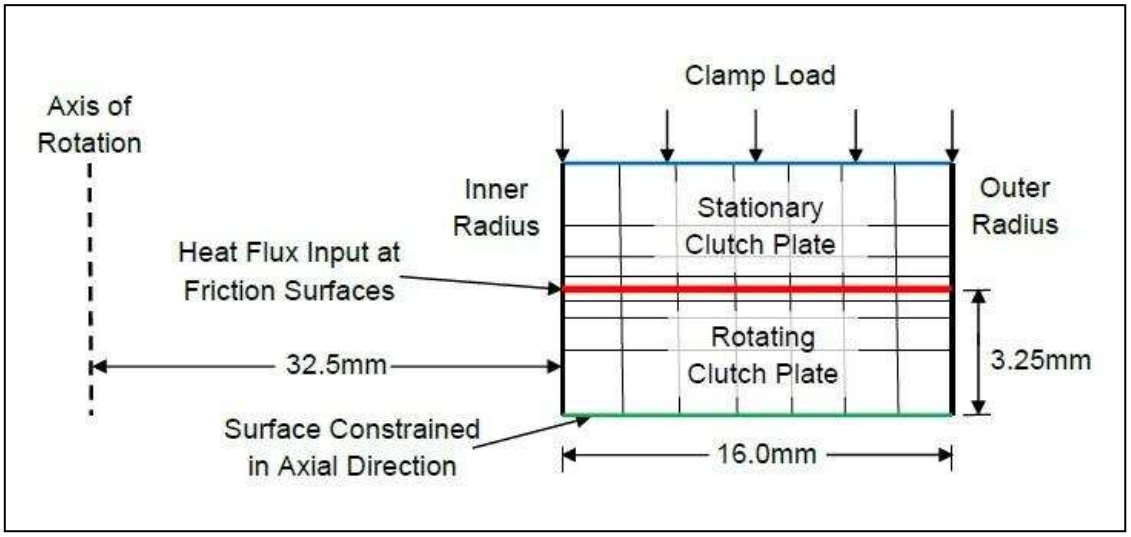

Figure 10 – Axisymmetric Finite Element Model of Clutch-Plate Pair

(Both clutch plates are 3.25mm thick)

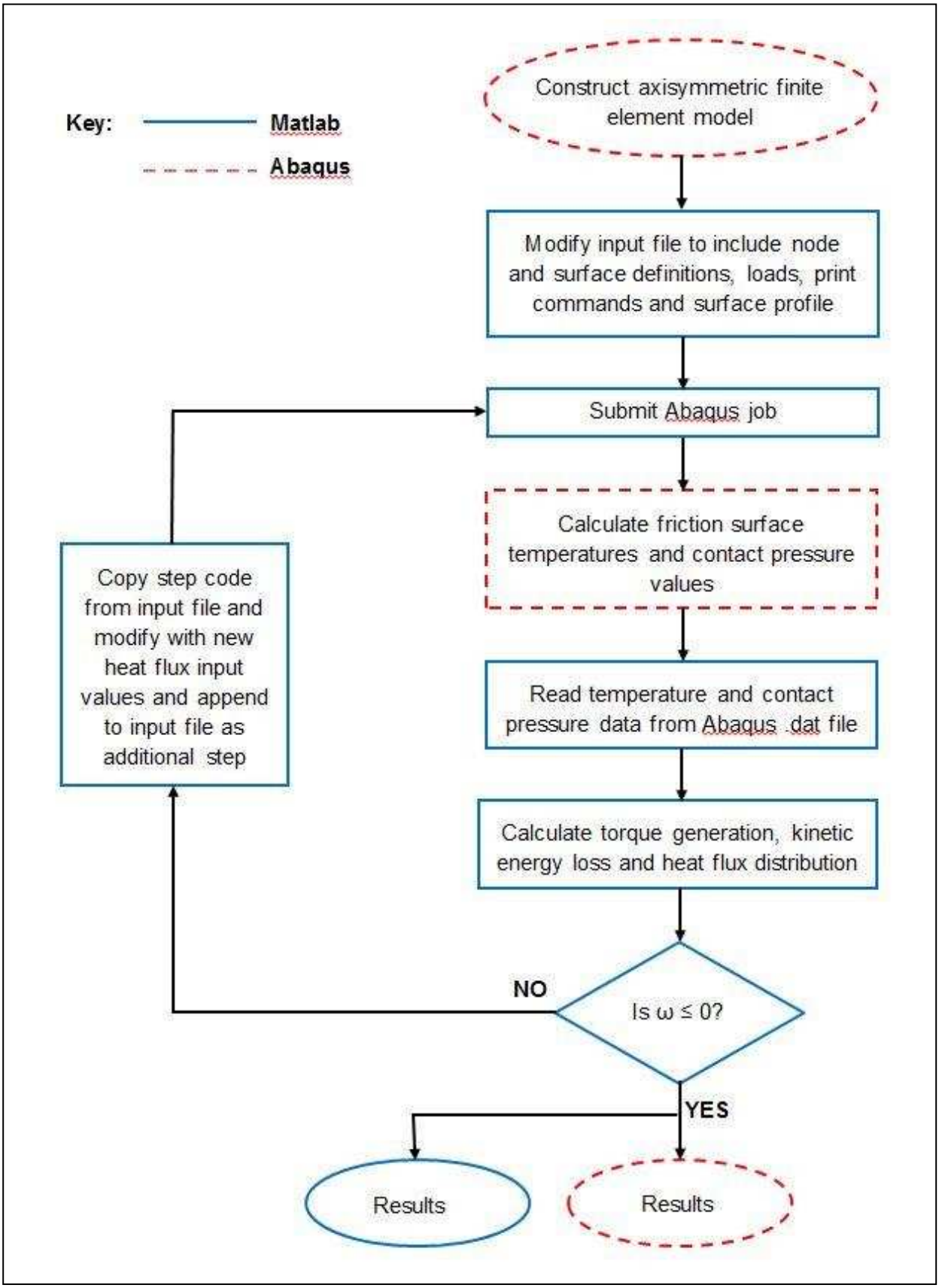

Figure 11 – Matlab-Abaqus Coupling for TCFEA

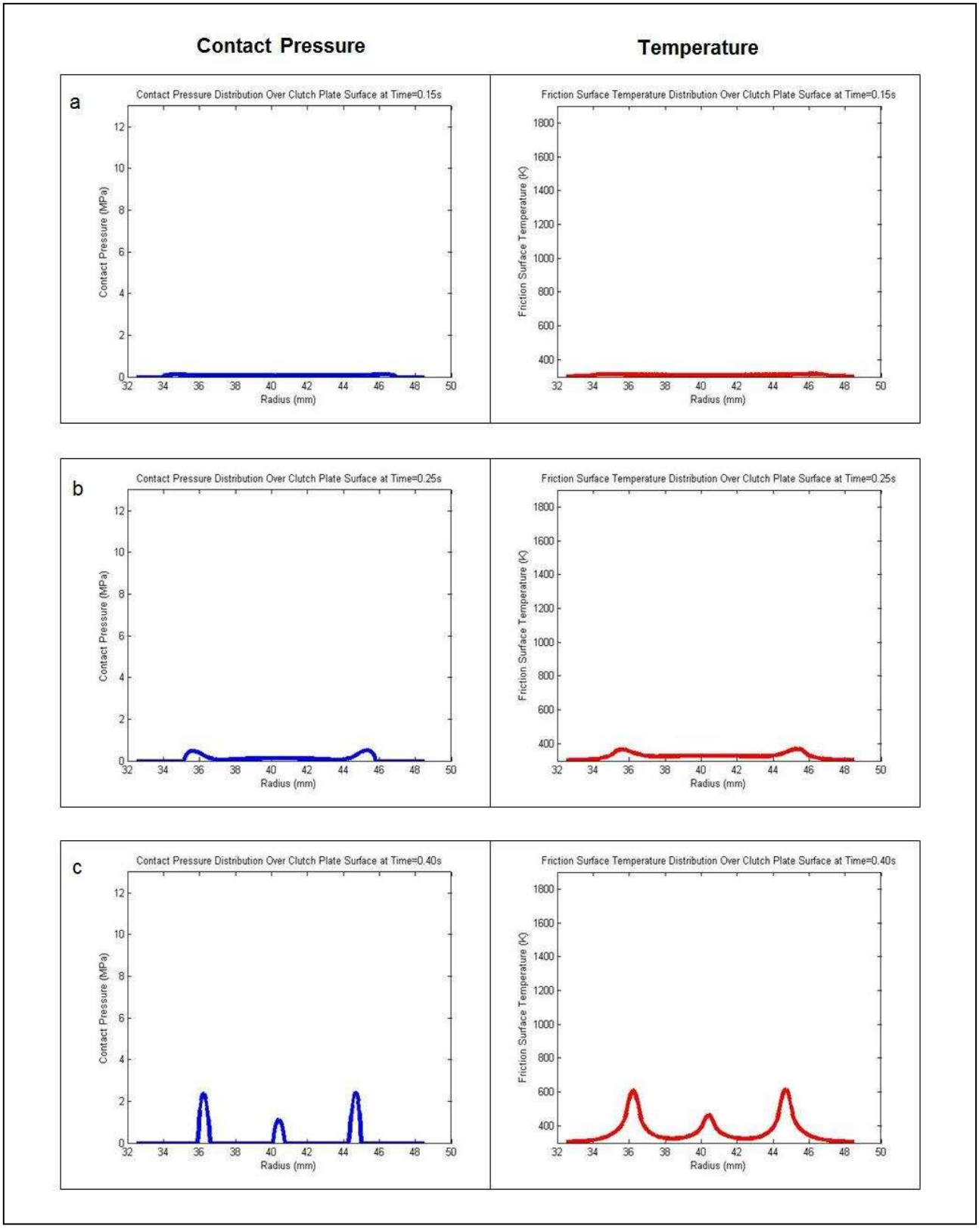

Figure 12 – Contact Pressure Distribution and Temperature Profile Across Friction Interface at (a) t=0.15s, (b) t=0.25s ad (c) t-0.40s (Non-Wear Model)

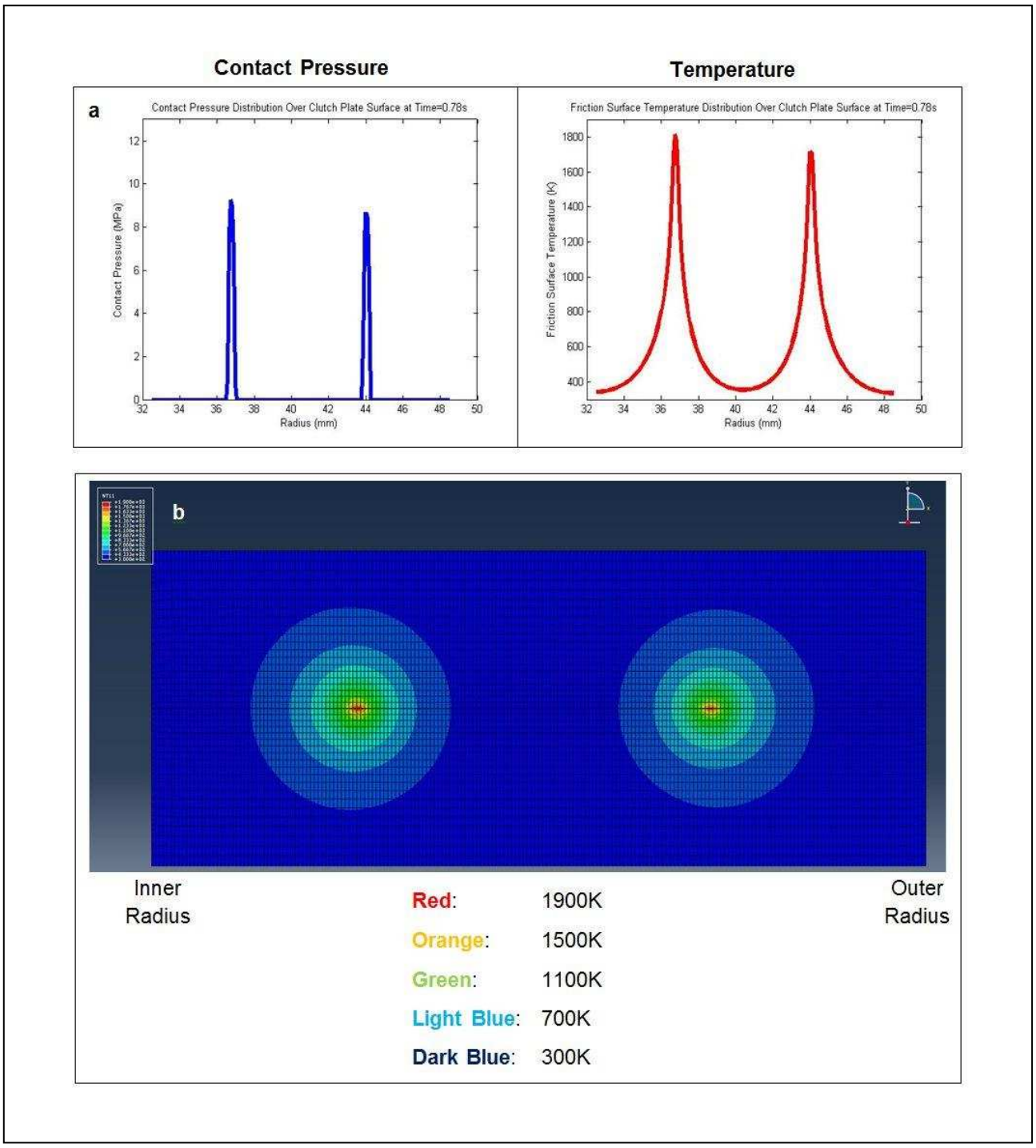

Figure 13 – (a) Contact Pressure Distribution and Temperature Profile at t=0.78s and (b) Temperature Contour Plot of Clutch Plates at t=0.78s (Non-Wear Model)

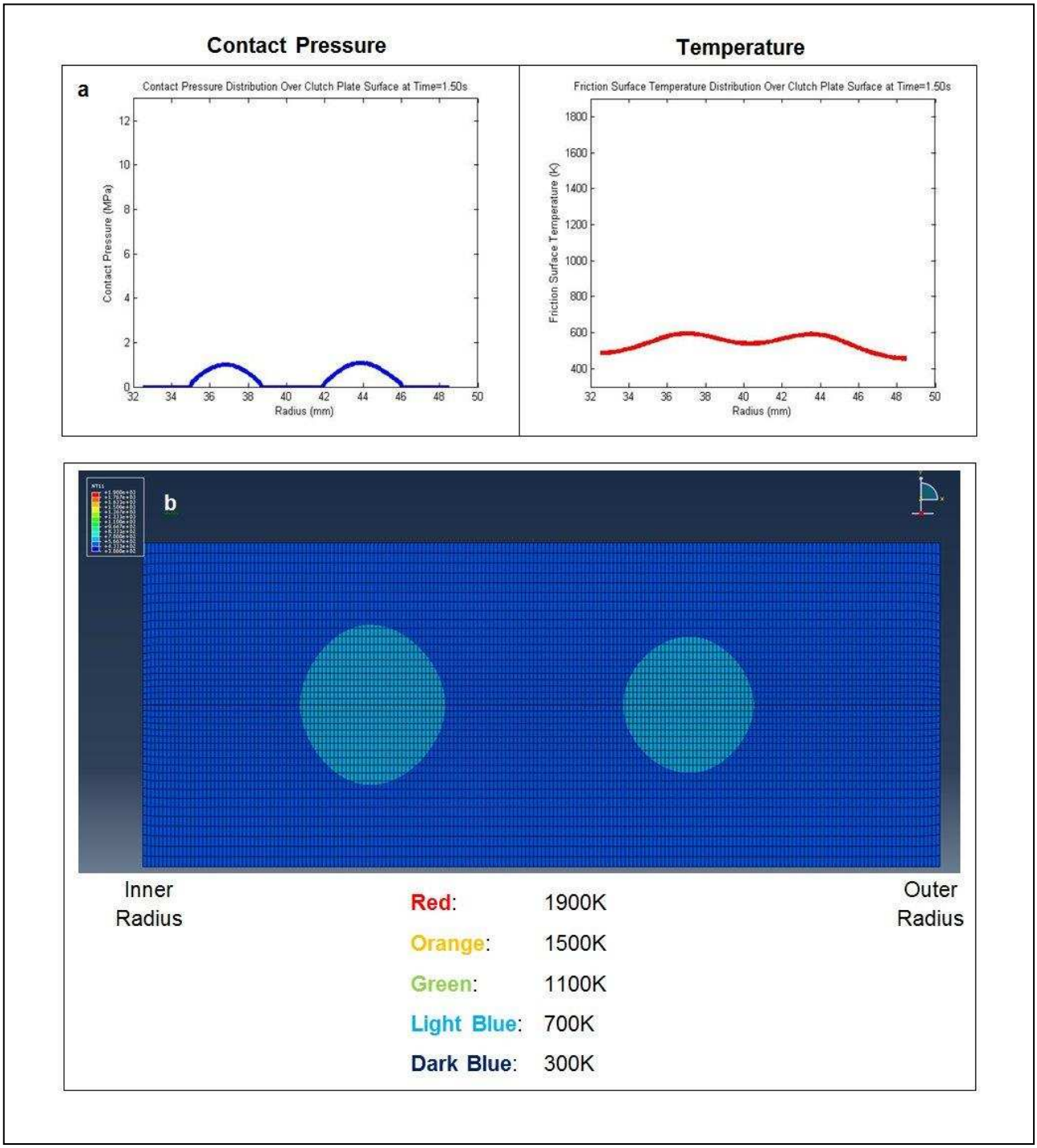

Figure 14 – (a) Contact Pressure Distribution and Temperature Profile at t=1.50s and (b) Temperature Contour Plot of Clutch Plates at t=1.50s (Non-Wear Model)

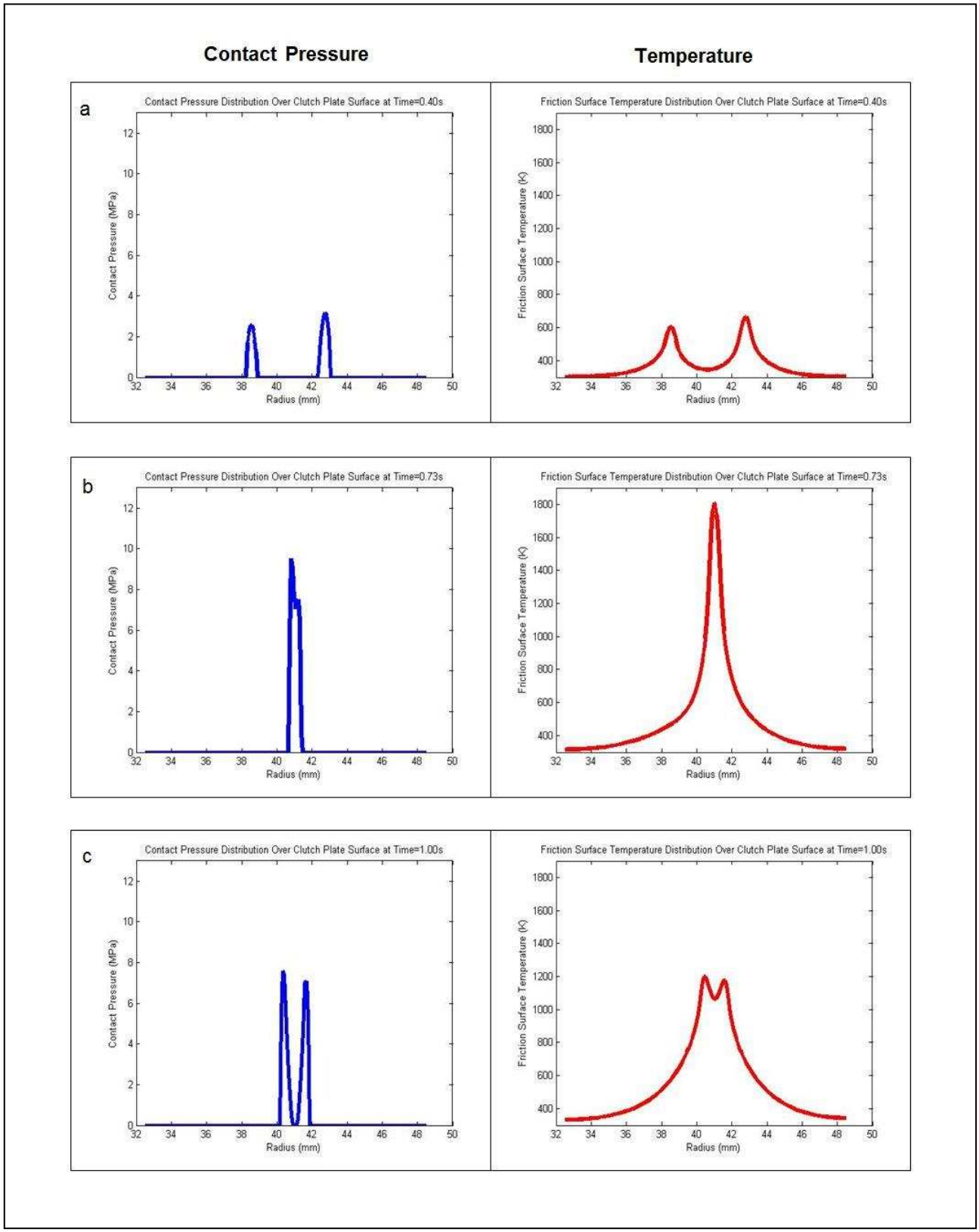

Figure 15 – Contact Pressure Distribution and Temperature Profile Across Friction Interface at (a) t=0.40s, (b) t=0.77s and (c) t=1.00s (Wear Model)

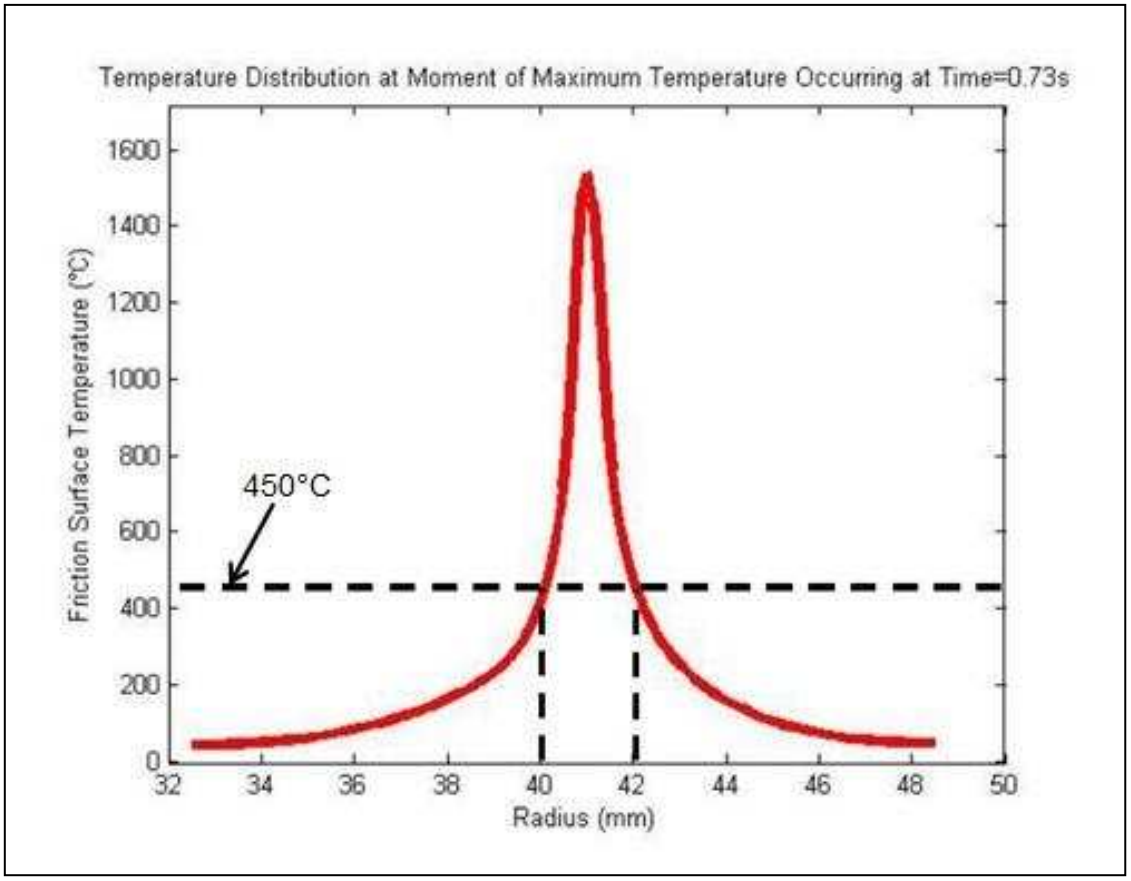

Figure 16 – Clutch-Plate Friction Surface Temperature Profile Predicted by TCFEA at t=0.73s at Which Maximum Temperature Occurs (Wear Model)